

## A New Layered Iron Arsenide Superconductor: (Ca,Pr)FeAs<sub>2</sub>

Hiroyuki Yakita,<sup>\*,†,||</sup> Hiraku Ogino,<sup>\*,†,||</sup> Tomoyuki Okada,<sup>†</sup> Akiyasu Yamamoto,<sup>†,||</sup> Kohji Kishio,<sup>†,||</sup> Tetsuya Tohei,<sup>‡</sup> Yuichi Ikuhara,<sup>‡</sup> Yoshito Gotoh,<sup>§,||</sup> Hiroshi Fujihisa,<sup>§</sup> Kunimitsu Kataoka,<sup>§</sup> Hiroshi Eisaki,<sup>§</sup> and Jun-ichi Shimoyama<sup>†,||</sup>

<sup>†</sup>Department of Applied Chemistry, The University of Tokyo, 7-3-1 Hongo, Bunkyo, Tokyo 113-8656, Japan

<sup>‡</sup>Institute of Engineering Innovation, The University of Tokyo, 2-11-16 Yayoi, Bunkyo, Tokyo 113-8656, Japan

<sup>§</sup>National Institute of Advanced Industrial Science and Technology (AIST), Tsukuba, Ibaraki 305-8565, Japan

### S Supporting Information

**ABSTRACT:** A new iron-based superconductor, (Ca,Pr)-FeAs<sub>2</sub>, was discovered. Plate-like crystals of the new phase were obtained, and its crystal structure was investigated by single-crystal X-ray diffraction analysis. The structure was identified as the monoclinic system with space group *P*2<sub>1</sub>/*m*, composed of two Ca(Pr) planes, Fe<sub>2</sub>As<sub>2</sub> layers, and As<sub>2</sub> zigzag chain layers. Plate-like crystals of the new phase showed superconductivity, with a *T*<sub>c</sub> of ~20 K in both magnetization and resistivity measurements.

Several groups of iron-based superconductors, such as REFeAs(O,F)<sup>1</sup> (*RE* = rare earth elements), AEF<sub>2</sub>AsF<sup>2</sup> (*AE* = alkaline earth metals), AEF<sub>2</sub>As<sub>2</sub>,<sup>3</sup> LiFeAs,<sup>4</sup> FeSe,<sup>5</sup> and compounds having perovskite-type oxide layers (e.g., Fe<sub>2</sub>P<sub>2</sub>Sr<sub>4</sub>Sc<sub>2</sub>O<sub>6</sub>),<sup>6</sup> have been discovered since 2008. There have been attempts at developing superconducting tapes and wires using potassium-doped AEF<sub>2</sub>As<sub>2</sub> and fluorine-doped REFeAsO, because of their high *T*<sub>c</sub> and high *H*<sub>c2</sub>. Nevertheless, the discovery of new superconductors with high *T*<sub>c</sub> and high chemical stability remains desirable. Since iron-based superconductors are composed of a stacking of superconducting layers of Fe<sub>2</sub>Pn<sub>2</sub> or Fe<sub>2</sub>Ch<sub>2</sub> (*Pn* = P, As, *Ch* = S, Se, Te) and blocking layers, designing and searching for new blocking layers are promising ways of discovering new superconductors. There are several compounds having anti-PbO type layers and As-based blocks, such as UCuAs<sub>2</sub>.<sup>7</sup> Recently two new iron-based superconductors, Ca<sub>10</sub>(Pt<sub>3</sub>As<sub>8</sub>)(Fe<sub>2</sub>As<sub>2</sub>)<sub>5</sub> and Ca<sub>10</sub>(Pt<sub>4</sub>As<sub>8</sub>)(Fe<sub>2</sub>As<sub>2</sub>)<sub>5</sub>,<sup>8–10</sup> were reported. These compounds have As-based blocking layers between Fe<sub>2</sub>As<sub>2</sub> layers. The structure of these compounds suggests the possibility of finding new iron-based superconductors with arsenide blocking layers. In addition, Saha et al. reported that single-crystalline (Ca,RE)-Fe<sub>2</sub>As<sub>2</sub> (*RE* = La, Ce, Pr, Nd) showed superconductivity with high *T*<sub>c</sub> (>40 K) in resistivity measurements.<sup>11</sup> Subsequently, superconductivity in RE-doped CaFe<sub>2</sub>As<sub>2</sub> has been reported by several groups.<sup>12</sup> On the other hand, several studies have reported the coexistence of two superconducting phases or interface superconductivity in this system.<sup>13,14</sup> Thus, a new superconducting phase is expected to emerge in the Ca-RE-Fe-As system.

In the present study, we have explored new iron-based superconductors in the Ca-Pr-Fe-As system and found a new

compound: (Ca,Pr)FeAs<sub>2</sub>. We report the crystal structure and physical properties of (Ca,Pr)FeAs<sub>2</sub>.

All samples were synthesized by a solid-state reaction, starting with FeAs(3N), PrAs(3N), Ca(2N), As(4N), and CaO(3N). Since the starting reagents PrAs and Ca are sensitive to the moisture and oxygen in air, manipulations were carried out in an argon-filled glovebox. Powder mixtures were pelletized, sealed in evacuated quartz ampules with alumina crucibles, and reacted at 1000–1200 °C for 24 h. The constituent phases were studied by powder XRD measurements using a RIGAKU Ultima-IV diffractometer, and the intensity data were collected in the 2θ range of 5–80° in increments of 0.02° using Cu Kα radiation. The local chemical composition of the samples was investigated by a scanning electron microscope (KEYENCE VE-7800) equipped with an energy dispersive X-ray spectrometer (EDX). The magnetic susceptibility was determined by a SQUID magnetometer (Quantum Design MPMS-XLSs). The electrical resistivity was measured by the AC four-point-probe method using a Physical Property Measurement System (Quantum Design). High-angle annular dark field (HAADF) images of the samples were obtained using a scanning transmission electron microscope (STEM: JEM-ARM200F, JEOL). In the structure analysis of (Ca,Pr)FeAs<sub>2</sub>, integrated intensity data were collected by a single-crystal X-ray diffractometer with an imaging plate (Rigaku R-Axis RAPID-II) using graphite-monochromatized Mo Kα radiation (λ = 0.71069 Å) at room temperature. In our data collection, 2518 reflections were measured, and 402 unique reflections with |*F*<sub>obs</sub>| > 3σ(|*F*<sub>obs</sub>|) were considered to correspond to the observed reflections. Lorentz polarization corrections and absorption corrections were applied to all of the collected reflections. All calculations for the structure analysis of (Ca,Pr)FeAs<sub>2</sub> were carried out using the computer programs Superflip<sup>15</sup> and FMLS<sup>16</sup>.

Figure 1 shows powder XRD patterns of (Ca<sub>0.9</sub>Pr<sub>0.1</sub>)-Fe<sub>1.9</sub>As<sub>2.1</sub>, (Ca<sub>0.9</sub>Pr<sub>0.1</sub>)Fe<sub>1.3</sub>As<sub>1.8</sub>O<sub>0.2</sub> and (Ca<sub>0.9</sub>Pr<sub>0.1</sub>)FeAs<sub>2</sub>, sintered at 1000–1200 °C. Diffraction peaks due to FeAs were observed in all samples. In addition, CaFe<sub>2</sub>As<sub>2</sub> and PrAs peaks appeared in (Ca<sub>0.9</sub>Pr<sub>0.1</sub>)Fe<sub>1.9</sub>As<sub>2.1</sub> and (Ca<sub>0.9</sub>Pr<sub>0.1</sub>)Fe<sub>1.3</sub>As<sub>1.8</sub>O<sub>0.2</sub>, and FeAs<sub>2</sub> was formed in the (Ca<sub>0.9</sub>Pr<sub>0.1</sub>)FeAs<sub>2</sub> sample. (Ca<sub>0.9</sub>Pr<sub>0.1</sub>)Fe<sub>1.3</sub>As<sub>1.8</sub>O<sub>0.2</sub> and (Ca<sub>0.9</sub>Pr<sub>0.1</sub>)FeAs<sub>2</sub> showed several

Received: October 28, 2013

Published: January 3, 2014

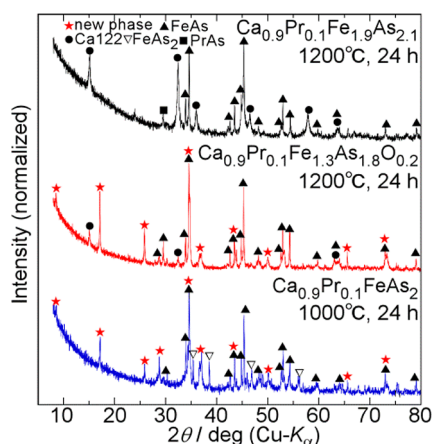


**Figure 1.** Powder XRD patterns of polycrystalline samples with the nominal compositions  $(\text{Ca}_{0.9}\text{Pr}_{0.1})\text{Fe}_{1.9}\text{As}_{2.1}$ ,  $(\text{Ca}_{0.9}\text{Pr}_{0.1})\text{Fe}_{1.3}\text{As}_{1.8}\text{O}_{0.2}$  and  $(\text{Ca}_{0.9}\text{Pr}_{0.1})\text{FeAs}_2$ .

unidentified peaks marked by stars in Figure 1, suggesting the generation of a new layered compound with a layer spacing of 10.4 Å. Note that the peaks appeared only in samples whose starting materials comprised iron-poor compositions relative to arsenic. Furthermore, we confirmed that Pr-doping was necessary to form the present new phase. Plate-like crystals of the new phase were successfully separated from a sintered bulk sample with a nominal composition of  $(\text{Ca}_{0.9}\text{Pr}_{0.1})\text{Fe}_{1.3}\text{As}_{1.8}\text{O}_{0.2}$ . The surface XRD patterns and an optical micrograph of a plate-like crystal are shown in Figure 2. The

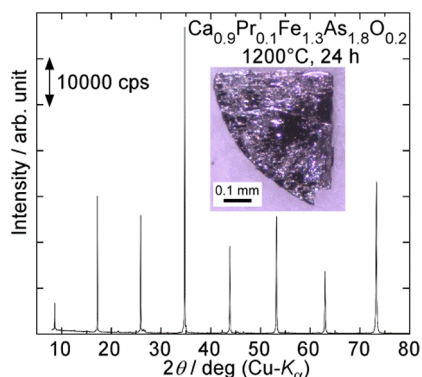


**Figure 2.** Surface XRD pattern of a plate-like crystal composed of the new phase. Inset shows an optical image of the sample.

edges of the crystals were slightly faceted as shown in the inset. All sharp peaks can be assigned to  $00l$  reflections if a layered crystal structure with an interlayer distance of 10.4 Å is assumed. Compositional analysis of such crystals by EDX indicated that their atomic ratio was  $(\text{Ca,Pr})/\text{Fe}/\text{As} = 24.1:23.5:52.4$ , which is close to  $(\text{Ca,Pr})/\text{Fe}/\text{As} = 1:1:2$ . The Pr concentration was about 17% of that of the Ca site. The addition of CaO promoted the formation of plate-like crystals, though oxygen could not be detected in the crystals by our EDX.

A single crystal of the new phase, approximately  $0.15 \times 0.12 \times 0.005$  mm in size, was used for the structural analysis. The analysis revealed the chemical formula of the new phase to be  $(\text{Ca}_{1-x}\text{Pr}_x)\text{FeAs}_2$ , consistent with the results of the compositional EDX analysis. Figure 3 shows the crystal structure of  $(\text{Ca}_{1-x}\text{Pr}_x)\text{FeAs}_2$ . The lattice constants of the monoclinic

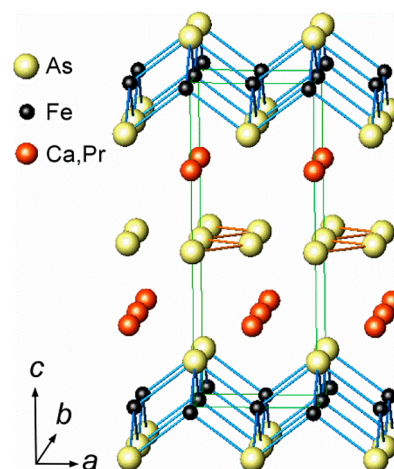


**Figure 3.** Crystal structure of  $(\text{Ca}_{0.73}\text{Pr}_{0.27})\text{FeAs}_2$  with monoclinic structure (space group  $P2_1/m$ ), as determined by single-crystal X-ray structure analysis.

structure of  $(\text{Ca}_{1-x}\text{Pr}_x)\text{FeAs}_2$  were refined to be  $a = 3.9163(8)$ ,  $b = 3.8953(7)$ ,  $c = 10.311(3)$  Å and  $\beta = 90.788(8)^\circ$ . We have observed the reflection condition for the  $0k0$  data to be  $k = 2n$ , and successfully obtained the centrosymmetric structure model defined by the space group  $P2_1/m$  for  $(\text{Ca}_{1-x}\text{Pr}_x)\text{FeAs}_2$ . The structure of  $(\text{Ca}_{1-x}\text{Pr}_x)\text{FeAs}_2$  was refined with 402 unique data. In the final refinement,  $(\Delta/\sigma)_{\text{max}} < 0.01$  was fully satisfied, where  $\Delta$  is the shift in the parameters, and  $\sigma$  is the standard uncertainty. The final atomic coordinates and equivalent isotropic displacement parameters are given in Table 1, where the  $R$  value converged

**Table 1.** Atomic Coordinates and Equivalent Isotropic Displacement Parameters ( $\text{Å}^2$ ) for  $(\text{Ca}_{0.73}\text{Pr}_{0.27})\text{FeAs}_2$

atom	occupancy	$x$	$y$	$z$	$100U_{\text{eq}}$ ( $\text{Å}^2$ )
Ca/Pr	0.730(8)/0.270	0.7432(9)	0.25	0.2297(5)	1.6(1)
Fe	1	0.255(1)	0.25	0.4977(6)	1.6(2)
As(1)	1	0.2460(7)	0.75	0.3598(4)	1.3(1)
As(2)	1	0.2193(8)	0.25	0.0023(4)	2.3(1)

to 0.116 and the  $R_w$  ( $w = 1/\sigma^2(F_{\text{obs}})$ ) value was 0.157. The Pr concentration obtained by structure analysis was 27% of the calcium site. Although this value is larger than that estimated by EDX analysis, both results suggested that the new phase had a higher Pr occupancy at the Ca site than the nominal ratio.

Figure 4, panels a and b, shows HAADF-STEM images of the plate-like sample with a nominal composition of  $(\text{Ca}_{0.9}\text{Pr}_{0.1})\text{FeAs}_2$ .

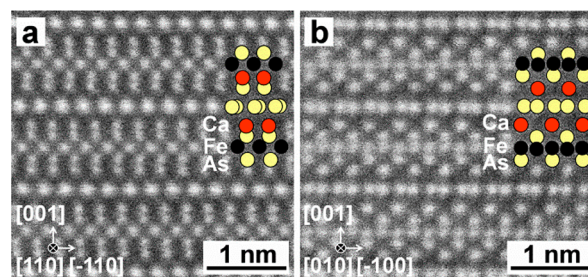


**Figure 4.** HAADF-STEM image of a plate-like crystal of  $(\text{Ca,Pr})\text{FeAs}_2$  observed from the  $[110]$  direction (a) and  $[010]$  direction (b).

$\text{Fe}_{1.3}\text{As}_{1.8}\text{O}_{0.2}$  taken from the [110] and [010] directions, respectively. As clearly seen, the observed crystal has a layered structure with an interlayer distance of approximately 10.4 Å, which corresponds well to the results of the structure analysis. A stacking of a  $\text{Fe}_2\text{As}_2$  layer, Ca(Pr) planes and  $\text{As}_2$  chain layers was clearly observed.

Figure 5 shows the temperature dependences of the zero-field cooled (ZFC) and field-cooled (FC) magnetization curves

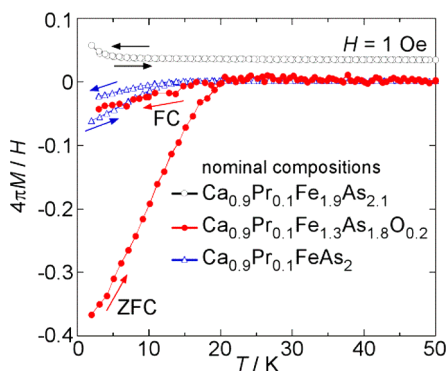


**Figure 5.** Temperature dependence of the ZFC and FC magnetization curves of  $(\text{Ca}_{0.9}\text{Pr}_{0.1})\text{Fe}_{1.9}\text{As}_{2.1}$ ,  $(\text{Ca}_{0.9}\text{Pr}_{0.1})\text{Fe}_{1.3}\text{As}_{1.8}\text{O}_{0.2}$  and  $(\text{Ca}_{0.9}\text{Pr}_{0.1})\text{FeAs}_2$ .

of a polycrystalline sample of  $(\text{Ca}_{0.9}\text{Pr}_{0.1})\text{Fe}_{1.9}\text{As}_{2.1}$  and a powder sample of  $(\text{Ca}_{0.9}\text{Pr}_{0.1})\text{FeAs}_2$ , and about ten plate-like crystals obtained from a sample with a nominal composition of  $(\text{Ca}_{0.9}\text{Pr}_{0.1})\text{Fe}_{1.3}\text{As}_{1.8}\text{O}_{0.2}$ . The typical crystal size was  $\sim 0.5 \times 0.5 \times 0.01$  mm and the magnetic field was applied normal to their wide surface. The sintered bulk samples of  $(\text{Ca}_{0.9}\text{Pr}_{0.1})\text{FeAs}_2$  quickly broke up into small pieces upon exposure to air, owing to air-sensitive impurities between the  $(\text{Ca,Pr})\text{FeAs}_2$  grains. Thus, their magnetization behavior was measured using a powder sample. Diamagnetism was not observed in the polycrystalline  $(\text{Ca}_{0.9}\text{Pr}_{0.1})\text{Fe}_{1.9}\text{As}_{2.1}$  sample. It indicates  $(\text{Ca,Pr})\text{Fe}_2\text{As}_2$  phase synthesized by the condition is not a superconductor. A large diamagnetism suggesting bulk superconductivity was observed in the samples containing the new phase,  $(\text{Ca}_{0.9}\text{Pr}_{0.1})\text{Fe}_{1.3}\text{As}_{1.8}\text{O}_{0.2}$ , with a  $T_{c(\text{onset})}$  of  $\sim 20$  K. For  $(\text{Ca}_{0.9}\text{Pr}_{0.1})\text{FeAs}_2$  powder, the relatively small diamagnetism observed does not disprove its bulk superconductivity, because the volume fraction of the new phase was small, as shown in Figure 1, and the grain size of the powder sample was comparable to the penetration depth.

Figure 6 shows the temperature dependence of the resistivity of a small plate-shaped bulk sample separated from a sintered bulk sample of  $(\text{Ca}_{0.9}\text{Pr}_{0.1})\text{Fe}_{1.3}\text{As}_{1.8}\text{O}_{0.2}$  that consists of plate-like crystals. In this measurement, an AC current was applied parallel to the wide plane of the sample and a magnetic field was applied normal to the wide surface. These experimental conditions mean that the AC current and magnetic field were applied, respectively, parallel and normal to the iron arsenide layer of the crystals of the new phase. A superconducting transition with a  $T_{c(\text{onset})}$  of  $\sim 24$  K was confirmed through resistivity measurements. However, this transition was relatively broad, and zero resistance was achieved at  $\sim 12$  K under zero external field. Since the current density in this measurement was less than  $0.1 \text{ A/cm}^2$ , this broad transition is presumably due to the distribution of  $T_c$  in the sample, reflecting an inhomogeneous praseodymium concentration and/or weak coupling between plate-like crystals in a small bulk sample.

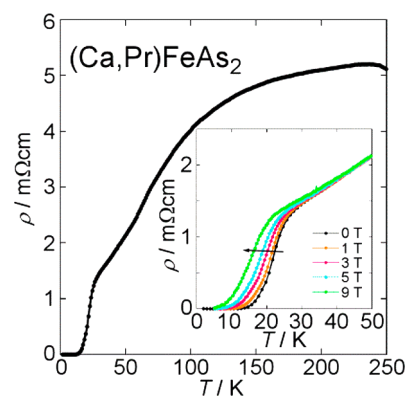


**Figure 6.** Temperature dependence of the resistivity of a polycrystalline sample of  $(\text{Ca}_{0.9}\text{Pr}_{0.1})\text{Fe}_{1.3}\text{As}_{1.8}\text{O}_{0.2}$  sintered at  $1200^\circ\text{C}$  for 24 h. The inset shows the resistivity under various magnetic fields; the arrow indicates the direction of increasing magnetic field.

Although slight increases in resistivity induced by an applied magnetic field can be confirmed up to  $\sim 40$  K, we believe this is not an intrinsic behavior of the new phase. This sample may contain very small amount of 40 K-class superconducting regions.

$(\text{Ca,Pr})\text{FeAs}_2$  did not show a 40 K-class high  $T_c$ . In  $\text{Ca}_{0.73}\text{Pr}_{0.27}\text{FeAs}_2$ , there are several As–Fe–As bond angles between  $106.2$  and  $111.2^\circ$  in the FeAs layer owing to its monoclinic structure. We tentatively attribute the 20 K-class  $T_c$  of  $(\text{Ca,Pr})\text{FeAs}_2$  to its As–Fe–As bond angles, because they are far from the ideal value of  $109.47^\circ$ . In As chain layers, the closest As–As distance is about  $2.60 \text{ \AA}$ , which is comparable to the As–As covalent bond distance ( $2.42 \text{ \AA}$ )<sup>17</sup> as well as to the distance between the  $[\text{As}_2^{4-}]$  dimers ( $2.50 \text{ \AA}$ ) in  $\text{Ca}_{10}(\text{Pt}_4\text{As}_8)(\text{Fe}_2\text{As}_2)_5$ ,<sup>9</sup> suggesting the presence of two As–As bonds for each As atom in this layer. In addition, the zigzag chain structure of pnictide is reported in several compounds such as  $\text{KAs}$ <sup>18</sup> and  $\text{SrZnSb}_2$ .<sup>19</sup> On the basis of these findings, we conclude that the valence of the As atom in the As chain layer is  $-1$ , which means that  $(\text{Ca,Pr})\text{FeAs}_2$  is composed of a stacking of a  $\text{Fe}_2\text{As}_2^{2-}$  layer, two  $\text{Ca}^{2+}$  planes, and a  $\text{As}_2^{2-}$  chain layer. Thus, hypothetical  $\text{CaFeAs}_2$  can be viewed as the parent compound of a new series of iron-based superconductors, and Pr substitution into the Ca site serves as electron doping. At present, we cannot control the Pr concentration in the compound, but if this is accomplished, the phase diagram of this compound can be obtained. Other challenges include optimization of the crystal structure and enhancement of  $T_c$  by varying the RE elements, for example. In addition, Katayama et al. have very recently reported a similar compound, although the chemical composition and crystal structure are slightly different.<sup>20</sup>

In summary, a new layered compound,  $(\text{Ca,Pr})\text{FeAs}_2$ , has been discovered in the Ca–Pr–Fe–As system. Plate-like crystals of this phase were obtained from a sample with a nominal composition of  $(\text{Ca}_{0.9}\text{Pr}_{0.1})\text{Fe}_{1.3}\text{As}_{1.8}\text{O}_{0.2}$  and a new crystal structure, composed of a  $\text{Fe}_2\text{As}_2$  layer, two Ca planes, and a  $\text{As}_2$  chain layer, was identified by X-ray diffraction analysis. EDX analysis indicated that the atomic ratio of the new phase is close to  $(\text{Ca,Pr})/\text{Fe}/\text{As} \approx 1:1:2$ . Atomic images of the samples obtained by HAADF-STEM observation were in good agreement with the results of structure analysis. Samples of the new phase exhibited superconductivity with a  $T_c$  of  $\sim 20$  K in both magnetization and resistivity measurements. The

discovery of this new compound demonstrated the variety of blocking layers in iron pnictides, and may lead to the discovery of other superconductors.

## ■ ASSOCIATED CONTENT

### ● Supporting Information

Crystallographic information for  $\text{Ca}_{0.73}\text{Pr}_{0.27}\text{FeAs}_2$  (CIF). This material is available free of charge via the Internet at <http://pubs.acs.org>.

## ■ AUTHOR INFORMATION

### Corresponding Authors

8757570603@mail.ecc.u-tokyo.ac.jp

tuogino@mail.ecc.u-tokyo.ac.jp

### Author Contributions

<sup>||</sup>H. Yakita, H. Ogino, A. Yamamoto, K. Kishio, Y. Gotoh and J. Shimoyama contributed to write this paper.

### Notes

The authors declare no competing financial interest.

## ■ ACKNOWLEDGMENTS

This study was supported by the Strategic International Collaborative Research Program (SICORP), Japan Science and Technology Agency, Asahi Glass Foundation and Tokuyama Science Foundation, and partly also by the “Nanotechnology Platform” (Project No. 12024046) of the Ministry of Education, Sports, Science and Technology (MEXT), Japan. We thank Prof. D. Johrendt for a valuable discussion on the synthesis of the samples.

## ■ REFERENCES

- (1) Kamihara, Y.; Watanabe, T.; Hirano, M.; Hosono, H. *J. Am. Chem. Soc.* **2008**, *130*, 3296.
- (2) Matsuishi, S.; Inoue, Y.; Nomura, T.; Yanagi, H.; Hirano, M.; Hosono, H. *J. Am. Chem. Soc.* **2008**, *130*, 14428.
- (3) Rotter, M.; Tegel, M.; Johrendt, D. *Phys. Rev. Lett.* **2008**, *101*, 107006.
- (4) Pitcher, M. J.; Parker, D. R.; Adamson, P.; Herkelrath, S. J. C.; Boothroyd, A. T.; Ibberson, R. M.; Bruneli, M.; Clarke, S. J. *Chem. Commun.* **2008**, 5918.
- (5) Hsu, F. C.; Luo, J. Y.; Yeh, K. W.; Chen, T. K.; Huang, T. W.; Wu, P. M.; Lee, Y. C.; Huang, Y. L.; Chu, Y. Y.; Yan, D. C.; Wu, M. K. *Proc. Natl. Acad. Sci. U.S.A.* **2008**, *23*, 14262.
- (6) Ogino, H.; Matsumura, Y.; Katsura, Y.; Ushiyama, K.; Horii, S.; Kishio, K.; Shimoyama, J. *Supercond. Sci. Technol.* **2009**, *22*, 075008.
- (7) Zolnieriek, Z.; Kaczorowski, D.; Troć, R. *J. Less-Common Met.* **1986**, *121*, 193.
- (8) Kakiya, S.; Kudo, K.; Nishikubo, Y.; Oku, K.; Nishibori, E.; Sawa, H.; Yamamoto, T.; Nozaka, T.; Nohara, M. *J. Phys. Soc. Jpn.* **2011**, *80*, 093704.
- (9) Ni, N.; Allred, J. M.; Chan, B. C.; Cava, R. J. *Proc. Natl. Acad. Sci. U.S.A.* **2011**, *108*, E1019.
- (10) Löhnert, C.; Stürzer, T.; Tegel, M.; Frankovsky, R.; Friederichs, G.; Johrendt, D. *Angew. Chem., Int. Ed.* **2011**, *50*, 9195.
- (11) Saha, S. R.; Butch, N. P.; Drye, T.; Magill, J.; Ziemak, S.; Kirshenbaum, K.; Zavalij, P. Y.; Lynn, J. W.; Paglione, J. *Phys. Rev. B* **2012**, *85*, 024525.
- (12) Lv, B.; Deng, L.; Gooch, M.; Wei, F.; Sun, Y.; Meen, J. K.; Xue, Y. X.; Lorenz, B.; Chu, C. W. *Proc. Natl. Acad. Sci. U.S.A.* **2011**, *20*, 15705.
- (13) Sun, Y.; Zhou, W.; Cui, L. J.; Zhuang, J. C.; Ding, Y.; Yuan, F. F.; Bai, J.; Shi, Z. X. *AIP Adv.* **2013**, *3*, 102120.
- (14) Wei, F. Y.; Lv, B.; Deng, L. Z.; Meen, J. K.; Xue, Y. Y.; Chu, C. W. [arXiv:1309.0034](https://arxiv.org/abs/1309.0034)
- (15) Palatinus, L.; Chapuis, G. *J. Appl. Crystallogr.* **2007**, *40*, 786.

- (16) Kato, K. *Acta Crystallogr.* **1994**, *A50*, 351.
- (17) Pyykkö, P.; Atsumi, M. *Chem.—Eur. J.* **2009**, *15*, 186.
- (18) Honle, W.; von Schnering, H. G. *Acta Crystallogr.* **1978**, *A34*, S152.
- (19) Brechtel, E.; Cordier, G.; Schaefer, H. Z. *Naturforsch., B* **1979**, *34*, 251.
- (20) Katayama, N.; Kudo, K.; Onari, S.; Mizukami, T.; Sugawara, K.; Sugiyama, Y.; Kitahama, Y.; Iba, K.; Fujimura, K.; Nishimoto, N.; Nohara, M.; Sawa, H. *J. Phys. Soc. Jpn.* **2013**, *82*, 123702.